

# Effects of giant laser pulses on a quasisteady plasma jet

S. I. Anisimov, V. A. Batanov, V. P. Gorkovskii, N. N. Zhukov, and V. P. Kopylov

*P. N. Lebedev Physics Institute, Academy of Sciences of the USSR, Moscow*

(Submitted 14 May 1982)

*Zh. Eksp. Teor. Fiz.* **83**, 1747–1755 (November 1982)

An investigation was made of the processes occurring in a quasisteady plasma jet formed above a solid target under the action of a neodymium laser pulse, which consisted of quasicontinuous lasing intervals as well as several “giant” peaks. A plasma-air contact interface was formed and shock waves, created in the plasma by the giant peaks, were reflected from this interface. An analysis of the reflection of shock waves led to a proposal for a new method for plasma diagnostics and measurements were made of the temperature in the jet. Low-threshold optical breakdown of air was observed near the contact surface.

PACS numbers: 52.75.Di, 52.70. — m, 52.35.Tc, 52.50.Jm

## §1. INTRODUCTION

One of the important tasks in the physics of the interaction of high-power radiation with matter is to study plasma jets formed as a result of high-temperature evaporation of condensed targets when they are subjected to laser pulses. Investigations carried out so far have made it possible to identify the main features of the physical processes occurring in jets under various irradiation conditions. For example, at moderate radiation flux densities  $\sim 10^6$ – $10^9$  W/cm<sup>2</sup> (such densities are typical of irradiation with neodymium glass lasers emitting relatively smooth millisecond pulses<sup>1</sup>) reaching a target, the flow of a plasma in a jet is established in a time much shorter than the duration of a laser pulse and a jet remains quasisteady throughout the laser pulse ( $\sim 10^{-3}$  sec). On the other hand, at high radiation flux densities (in excess of  $10^{10}$  W/cm<sup>2</sup>), typical of Q-switched lasers emitting pulses lasting tens of nanoseconds, the flow of a plasma in a jet is transient and it gives rise to transient ionization fronts (shock and optical detonation waves).<sup>2</sup>

We investigated the formation and motion of a plasma under more complex irradiation conditions, when a target is subjected simultaneously to a smooth millisecond pulse and a sequence of three or four giant pulses of about 100 nsec duration.<sup>1</sup> This “hybrid” irradiation regime was obtained when a neodymium laser with a plasma mirror was used.<sup>3</sup> A study was made of the evaporation of a graphite target in atmospheric air. The smooth part of the laser pulse generated a quasisteady jet near the target surface. The boundary between this jet and air (which was a discontinuous contact surface) remained practically immobile (relative to the target) throughout the main part of the pulse. The giant pulses or spikes created shock waves at the target surface and these traveled along the jet plasma, reached the boundary with air, and were reflected from it. We found that the measured velocity of the reflected shock wave could be used to calculate the plasma temperature in the quasisteady jet as well as the temperature of the layer adjoining the jet.

We found that giant pulses caused optical breakdown of air near the contact boundary with the plasma. The threshold density of the radiation flux needed for this breakdown was between two and three orders of magnitude less than the values reported earlier<sup>4–6</sup> for the breakdown of cold air far

from such boundaries. The likely mechanisms of this reduction in the breakdown threshold are considered briefly in the final section (§3).

## §2. LASER PARAMETERS, TARGET IRRADIATION CONDITIONS, RECORDING METHODS

Our experiments were carried out using a neodymium laser consisting of four GOS-1000 illumination enclosures. A detailed description of the apparatus was given in Ref. 3. The laser generated a beam with an outer diameter of 4.5 cm and the total radiation energy per pulse was 280–300 J. The shape of the laser pulses was typically of the kind shown in Fig. 1. Measurements of the radiation energy in the smooth parts of a laser pulse as well as at the giant peaks were made for each separate pulse employing a method described in Ref. 3. The average power during the quasisteady part of the laser pulse had maximum values of 0.8–1.0 MW at the beginning of the pulse and fell at its end. At the moment corresponding to the last giant peak the average power of the quasisteady radiation was 10–20% of the maximum value. The shape of the quasisteady component of the pulse was reproducible from one shot to another.

The energy of the giant peaks ranged from 20 to 60 J. These peaks had a fine time structure due to mode locking. They consisted from between one and three trains of short spikes of less than 5 psec duration (Ref. 7).<sup>2</sup> The interval between these spikes was 8.8 nsec. Each giant peak consisted of from 15 to 50 picosecond spikes, and its total duration was between 160 and 480 nsec. The maximum value of the power during the picosecond spikes was at least 200 GW.

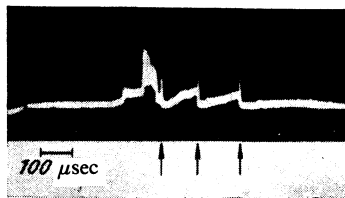


FIG. 1. Typical oscillogram of a laser pulse. The arrows identify the positions of the giant peaks. The vertical scale selected in this oscillogram is insufficient to show the full amplitude of these peaks.

Our experiments were carried out on targets made of graphite and these were irradiated in air at atmospheric pressure. A laser beam was focused on the target surface by a lens with a focal length of 50 cm. The angular divergence of the beam, measured in Ref. 7, was  $2 \times 10^{-4}$  rad. Therefore, the diameter of the focal spot on the target surface was  $10^{-2}$  cm and the density of the radiation flux in this spot was  $10^9$ – $10^{10}$  W/cm<sup>2</sup> during the quasisteady lasing and  $10^{15}$ – $10^{16}$  W/cm<sup>2</sup> during the picosecond spikes. Such irradiation produced a crater about 1 mm in diameter and 3 mm deep in the graphite target.

The processes in the plasma jet were investigated by high-speed photography. The radiation was recorded on a millisecond time scale using an SFR high-speed camera, whereas in the nanosecond range we employed an Agat-SF image-converter camera. Both were used in the streak (scanning) mode. The motion of a luminous plasma along the laser beam axis was recorded on a photographic film.

### §3. GASDYNAMICS OF A PLASMA JET. LOW-THRESHOLD BREAKDOWN OF AIR

A typical large-scale pattern of the plasma motion in a jet is shown in a streak photograph in Fig. 2, obtained with the SFR camera. The streak pattern was "locked" in time to the corresponding laser pulse. A steady structure of the jet was established soon after the beginning of evaporation of the target under the action of the smooth part of the laser pulse and the formation of a plasma. This structure was reproducible from one shot to another. Shock waves traveling toward the laser appeared in the steady-state plasma near the target under the action of the giant peaks. When these waves reached the contact surface between the plasma and air, they were reflected back toward the target. We shall analyze below the characteristics of the quasisteady structure of the jet, propagation of shock waves in the jet plasma, and data on the optical breakdown of air near the boundary with the plasma.

1. The gasdynamics of the evaporation of graphite under the action of quasicontinuous optical radiation in our experiments is in many respects analogous to the gasdynamics of evaporation of metal targets by millisecond laser pulses.<sup>1</sup> Streak photographs recorded near the target surface show clearly a dark space, representing a zone of adiabatic expansion of vapors, and a luminous front of a static change in the density separated from the target by 1–2 cm. In time-integrated photographs of the plasma jet this density discontinuity is, as in Ref. 1, a luminous sphere in contact with the irradiated region of the target. The complete analogy between the structure of the plasma flow observed in Ref. 1 and in the present study allows us to employ a simple formula from Ref. 1, which relates the temperature to the plasma flow velocity directly behind the density discontinuity front:

$$\frac{kT}{m} = \frac{\gamma+1}{2(\gamma-1)^2} v^2$$

( $m$  is the atomic mass,  $k$  is the Boltzmann constant,  $\gamma$  is the adiabatic exponent assumed in the estimates below to be 5/3). The experimentally determined velocity  $v$  is a function of the radiation power density in the smooth part of a laser pulse. It is maximal at the beginning of the pulse and falls toward its end. The average values of the velocity deduced from the streak photographs are  $v_i = (3.3 \pm 0.3) \times 10^5$  cm/sec at the beginning of a pulse and  $v_f = (1.9 \pm 0.2) \times 10^5$  cm/sec at the end of a pulse. This corresponds to the following initial and final values of the temperature on the jet axis immediately behind the static density discontinuity front:  $T_i = (45 \pm 9) \times 10^3$  K and  $T_f = (15 \pm 2) \times 10^3$  K.

It is shown in Ref. 9 that away from the density discontinuity front at distances comparable with the size of the adiabatic expansion zone the plasma temperature falls by a factor of 1.5–3. In our experiments the temperature in the peripheral part of the jet was also considerably less than the temperature at the density discontinuity front and at the periphery it amounted to  $(10 - 7) \times 10^3$  K.

During the initial stage of a laser pulse the flux of the evaporated matter comes into contact with the surrounding atmosphere and drives air away from the target surface (Fig. 2). During a pulse of  $\sim 10^{-3}$  sec duration there is no significant mixing of the plasma with air. The outer boundary of the plasma moves away from the target by 8–9 cm and remains at this distance throughout the subsequent part of the pulse. The slowing down of the contact boundary is due to an increase in the volume of the jet and the simultaneous reduction in the density of the flux of matter evaporated from the target surface.

The pressures on both sides of the contact surface are the same (and they amount to 1 atm), but the temperatures differ by an order of magnitude. Consequently, a density discontinuity appears at the contact surface and this is the reason for the reflection of shock waves from the outer

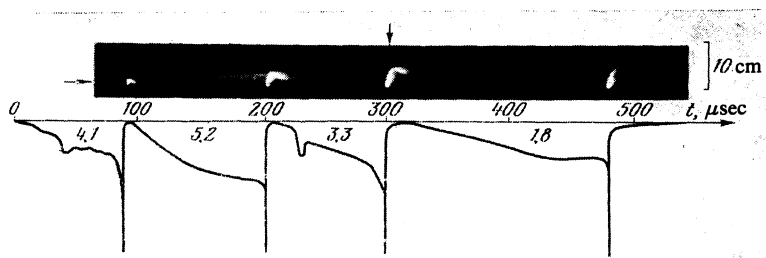


FIG. 2. Streak photographs of a plasma jet and profile of a laser pulse. The time is measured from the beginning of the pulse. The numbers in the oscillogram give the average values of the power density (in gigawatts per square centimeter) on the target surface. The vertical lines in the oscillogram are the giant peaks. The vertical arrow at the top identifies the direction of the laser beam and the horizontal arrow gives the target position.

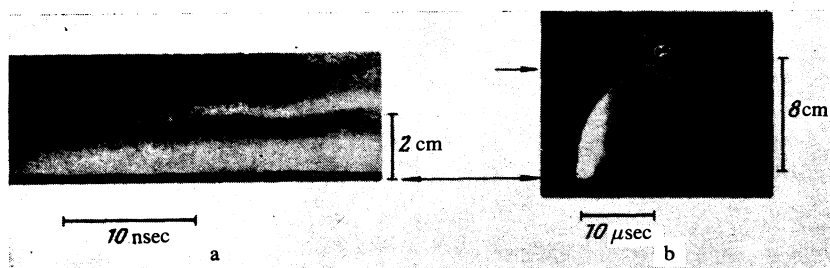


FIG. 3. Streak photographs of the appearance and propagation of a shock wave front: a) recorded with an image-converter camera; b) recorded with an SFR high-speed camera. The laser beam was directed downward; the time is measured from left to right and the position of the target is identified by the lower arrow. The upper arrow in Fig. 3b identifies the position of the contact boundary.

boundary of the plasma jet (Fig. 2). We shall show below that a shock wave in the surrounding air is also created as a result of such reflection.

2. We shall consider the processes of formation and propagation of shock waves in a quasisteady plasma jet. The formation of a shock wave under the action of a giant laser peak occurs behind the front of the static density discontinuity located at a distance of about 2 cm from the target surface (Fig. 3a). Initially, the motion of such a shock wave is maintained by the absorption of energy from the laser beam at the wave front. This is indicated by the wave-like nature of the motion of the front whose period is equal to the interval separating picosecond spikes. In the photograph in Fig. 3a we can see that the front of a shock wave is displaced as a whole over a distance of 1.7 cm in a time of 70 nsec so that the average velocity of this front is  $\approx 2.5 \times 10^7$  cm/sec. At the end of a giant peak the shock wave velocity decreases in a time interval of the same order as the peak duration and this is manifested as a kink in the slope of the luminous front (relative to the time axis) in the large-scale streak photographs of the kind shown in Fig. 3b. Shock waves reach the air-plasma contact surface at velocities of  $10^5$ – $10^6$  cm/sec. The scatter of the shock wave velocities is due to the scatter of the energy and time parameters of the giant peaks mentioned in §2. We determined the ratio of the velocities of shock waves incident on the contact surface  $D_i$  and those reflected from it  $D_r$ . The experimental dependence  $D_r(D_i)$  was found to be very weak: a change in  $D_i$  by an order of magnitude altered  $D_r$  by a factor of just 1.6. This result is explained in a theoretical analysis given in §4. If we consider the process of reflection of shock waves, we can show that the velocity  $D_r$  is governed mainly by the plasma temperature. This important conclusion will be used by us later to find the plasma jet temperature.

A diagnostic method proposed in §4 can be used, in principle, to determine not only the plasma temperature but also the temperature of air near the jet boundaries from the velocity  $D_r$  of the shock waves traveling in air. However, the technical aspects of the recording method employed by us made it impossible to carry out detailed measurements of the velocity of propagation of shock waves in air. In the whole series of experiments, only in the case of a few giant peaks were we able to record weak radiation from a shock wave in air near the air-plasma contact surface and to measure the

velocity of such a shock wave (the second giant peak from the beginning of a laser pulse shown in the streak photograph of Fig. 2 was one of the few such cases when the measurements were possible). The measured velocities  $D_r$  were 550–750 cm/sec. In view of the small amplitude of the shock waves in air (see §4), these values of  $D_r$  corresponded to temperatures of  $T_{O_2} \approx 850$ – $1550$  K. Heating of the adjoining air layer could be due to the absorption of the ultraviolet component of the plasma radiation.<sup>10</sup> This hypothesis seems to be very likely to be correct if we allow for the frequency dependence of the absorption coefficient of air in the ultraviolet region. Some role in the heating of air may also be played by the mechanism of electronic heat conduction out of the plasma.

3. Before we consider the problem of reflection of shock waves, we shall describe briefly another interesting physical effect observed in our experiments. Low-threshold optical breakdown of air by picosecond laser pulses was observed near the air-plasma contact surface (Fig. 4). This breakdown occurred in about 30% of all the streak photographs and it was manifested by a bright flash in air, which appeared at the moments of generation of trains of picosecond spikes; it was located at a distance 4–10 cm from the target surface and 1–2 cm from the air-plasma contact surface.

The optical breakdown threshold of atmospheric air at the wavelength of  $1.06 \mu$  was  $3 \times 10^{14}$  W/cm<sup>2</sup> for the picosecond spikes.<sup>4</sup> In our experiments the intensity of laser radiation in the breakdown region was two or three orders of magnitude less.

As demonstrated by the photographs in Fig. 4, the breakdown of air occurred well before the shock wave reached the air-plasma contact surface. Hence, it was clear that this low-threshold breakdown was in no way related to the shock wave. According to the results of many investigations of the mechanisms of low-threshold breakdown (see, for example, Ref. 11), initiation of such breakdown is in one way or another related to the processes that occur on the target surface. In our experiments the low-threshold breakdown is clearly associated with the proximity of the air-plasma contact surface. Reduction in the breakdown threshold may be due to several factors. First, the density of free electrons in air near the contact surface increases because of the diffusion of electrons out of the plasma. An estimate of the distance in which electrons can travel into the atmospheric air by diffusion in a time of  $\sim 10^{-3}$  sec gives approximately 1

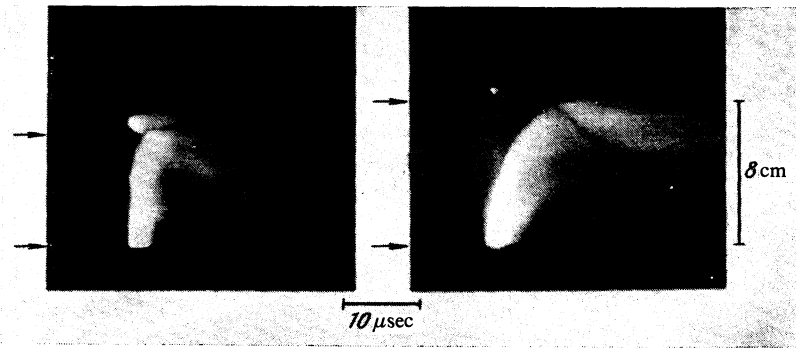


FIG. 4. Parts of streak photographs showing the low-threshold optical breakdown of air. The positions of the target and of the air-plasma boundary are identified by horizontal arrows. The laser pulse is incident in the downward direction.

cm, which is not in conflict with the results of our observations.

Second, as pointed out earlier, preliminary ionization of air in the breakdown region may be due to the ultraviolet component of the radiation emitted by the plasma jet.

Finally, we cannot exclude the possibility of ionization of air by the hard x rays emitted from the high-temperature plasma layer on the target surface at the moment of interaction with a giant peak.<sup>12</sup> Further investigations are needed in order to determine the influence of each of these mechanisms.

#### §4. REFLECTION OF SHOCK WAVES FROM THE AIR-PLASMA CONTACT SURFACE

We shall establish the relationship between the parameters of the incident and reflected shock waves in the vicinity of the air-plasma contact surface simply by considering the one-dimensional problem of decay of a discontinuity.<sup>13</sup> Figures 5a and 5b show the profiles of the pressure before and after reflection, and they explain the notation used below. The indices  $i$ ,  $r$ , and  $t$  refer to the incident, reflected, and transmitted waves, respectively; the index 0 denotes the initial values of the parameters; the indices 1 and 2 refer to the plasma and the surrounding air, respectively. All the relationships are valid in the laboratory coordinate system in which the air-plasma contact surface (identified by crosses in Fig. 5) is initially at rest. As a result of the interaction with a shock wave the contact boundary acquires a velocity  $u_b$ . Naturally, we have  $u_r = u_t = u_b$  and  $p_t = p_r$  because of the continuity of the normal velocity and pressure across the contact boundary.

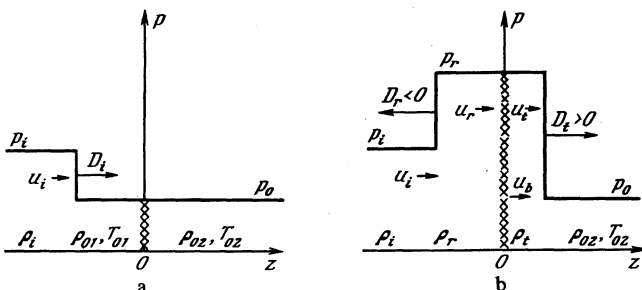


FIG. 5.

Writing down the equation for the shock adiabat of a reflected wave in the form

$$^{3/2}(p_r/\rho_r - p_i/\rho_i) = ^{1/2}(p_r + p_i)(1/\rho_i - 1/\rho_r),$$

we obtain

$$p_r/p_i = (3 + \alpha_1)/(3 - 4\alpha_1), \quad (1)$$

where  $\alpha_1 = 1 - \rho_i/\rho_r$ . Similarly, we obtain the following relationship from the equation for the shock adiabat for the transmitted wave:

$$p_r/p_0 = (5 + \alpha_2)/(5 - 6\alpha_2), \quad (2)$$

where  $\alpha_2 = 1 - \rho_0/\rho_t$ . The equations of continuity of the mass and momentum fluxes yield the following equations after some simple transformations:

$$(p_r - p_i)/\rho_i u_i^2 = (1 - x)^2/\alpha_1, \quad (3)$$

$$(p_r - p_0)/\rho_0 u_i^2 = x^2/\alpha_2, \quad (4)$$

$$p_i/p_0 = (5 - \kappa)/4\kappa, \quad (5)$$

$$(p_i - p_0)/\rho_i u_i^2 = (1 + 3\kappa)/3(1 - \kappa). \quad (6)$$

Here,  $\kappa = M_i^{-2}$ ;  $M_i = D_i/c_{01}$  is the Mach number of the incident wave;  $u_i = 3/4D_i(1 - \kappa)$  is the mass velocity;  $x = u_b/u_i$ .

In the above relations the unknowns are the parameters of the transmitted and reflected waves:  $p_r$ ,  $x$ ,  $\alpha_1$ , and  $\alpha_2$ . They are in fact given by Eqs. (1)–(4), whereas Eqs. (5) and (6) relate the known quantities describing the incident wave. We can easily see that  $p_r$  and  $x$  can be eliminated from Eqs. (1)–(4), so that we are left with a system of two equations describing  $\alpha_1$  and  $\alpha_2$  as functions of the Mach number of the incident wave. However, it is in practice more convenient to use a different approach. Solving the system (1)–(4) for  $x$ , we obtain

$$x = (\beta - 1)^{-1} \{ [\beta + (\beta - 1)\alpha_1(1 + 3\kappa)/3(1 - \kappa)]^{1/2} - 1 \}, \quad (7)$$

where  $\beta = \alpha_1(1 + 3\kappa)/4\alpha_2\omega$ ,  $\omega = \rho_{01}/\rho_{02}$  is the initial ratio of the densities at the air-plasma boundary. It follows from the above that  $\omega \ll 1$  and, therefore, we find from Eq. (7) that  $x \sim \omega^{1/2} \ll 1$ . This means that the velocity of the contact surface is considerably less than the mass velocity of the plasma in the incident wave. Using the smallness of  $x$ , we can readily obtain an iteration solution of the problem in accordance with the following procedure. When a known approximate value of  $x$  is available, we can calculate  $\alpha_1$  from

$$\alpha_1 = 6q[(1+1/4q)^{1/2} - 1], \quad q = [(1-\kappa)(1-x)]^2 / (\bar{\nu}-\kappa)(1+3\kappa).$$

We can then determine  $\alpha_2$ :

$$\alpha_2 = \frac{5(\mu-1)}{6\mu+1}, \quad \mu = \frac{3+\alpha_1}{3-4\alpha_1} \frac{\bar{\nu}-\kappa}{4\kappa},$$

which is followed by the calculation of  $\beta$  and refinement of the value of  $x$  in Eq. (7).

Noting that

$$\omega = \frac{\rho_{01}}{\rho_{02}} = \frac{m_1 T_{02}}{m_2 T_{01}} = \frac{\gamma_1 R T_{02}}{m_2} \frac{1}{\kappa D_i^2},$$

where  $m_1$  and  $m_2$  are the molecular weights of the plasma and air, and  $R$  is the universal gas constant, we find that  $\omega\kappa = \text{const}/D_i^2$ . A calculation carried out in accordance with the above procedure gives therefore the ratio  $D_r/D_i$  as a function of  $\kappa$  for a given value of  $\omega\kappa$ . It should be noted that in the case of significant ionization of the plasma the value of  $m_1$  should be replaced with  $m_1^* = m_1/(Z+1)$ , where  $Z$  is the average charge of an ion.

The results of a numerical calculation of the dependence of  $D_r/c_{01}$  on  $M_i$  for various temperatures  $T_{01}$  and two values of  $T_{02} = 300$  and  $1500$  K are plotted in Fig. 6. We can see that for Mach numbers  $M_i$  smaller than a certain value  $M_i^*$  the ratio  $D_r/c_{01}$  varies little when is varied and remains close to unity. The value of  $M_i^*$  increases on reduction in  $T_{01}$  and on increase in  $T_{02}$ . Therefore, the experimentally observed (see §3) weak dependence of  $D_r$  on  $D_i$  means that  $D_r$  can be regarded quite accurately as equal to the velocity of sound  $c_{01}$  in the unperturbed plasma. This provides a convenient method of estimating the plasma temperature near its boundary with air.

The experimental dependences of  $D_r$  on  $D_i$  are compared in Fig. 7 with the theoretical curves plotted for  $T_{02} = 1500$  K. The circles are the results of measurements carried out during the first two (counting from the beginning of a laser pulse) giant peaks, whereas triangles represent the results obtained for the third and fourth peaks. The agreement between the experimental data and the calculated curves in Fig. 7 shows that the plasma temperature during the first half of the laser pulse was  $10\,000$  K, whereas during the second half it was  $7000$  K. Cooling of the peripheral part of the jet with time, deduced from the velocity of the reflected shock waves, was in qualitative agreement with the corre-

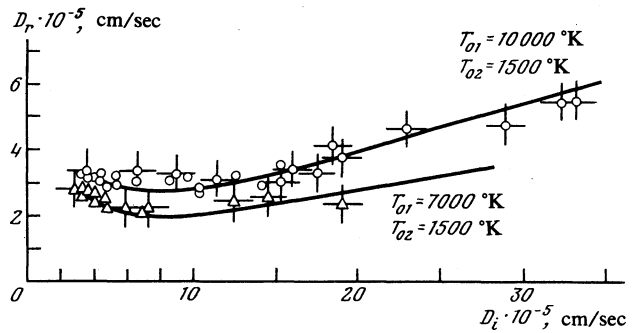


FIG. 7.

sponding estimates of the plasma temperature near the target behind the front of the static density discontinuity, reported in §3.

One should also point out that a comparison of the experimental results with the calculated curves (Fig. 7) made it possible to establish reliably not only the plasma temperature, but also the temperature of the air layer in contact with the jet. The value  $T_{02} = 1500$  K, found from the ratio of the velocities  $D_r$  and  $D_i$ , was not in conflict with the data given in §3 on the velocity of the shock waves in air.

## §5. CONCLUSIONS

We investigated the physical processes in a quasisteady plasma jet acted upon by giant laser radiation peaks. We studied the steady-state structure of the jet, observed shock waves traveling along the plasma, and recorded their reflection from the contact boundary between the plasma and air. We estimated the temperature of the jet near the target and in its peripheral region during the initial and final parts of the laser radiation pulses. We made a theoretical analysis of the reflection of shock waves from the plasma-air boundary. The results of this analysis were used to propose a new method for the diagnostics of a plasma and of an air layer adjoining it. The advantages of this method are its simplicity and effectiveness. It makes it possible to determine simultaneously the temperature of a quasisteady plasma and of the surrounding gaseous medium with a sufficiently high time resolution. It should be pointed out that shock waves in a plasma can, in principle, be excited also by an external laser source emitting giant pulses. The range of applications of the proposed method is not limited to laser plasmas, but can be

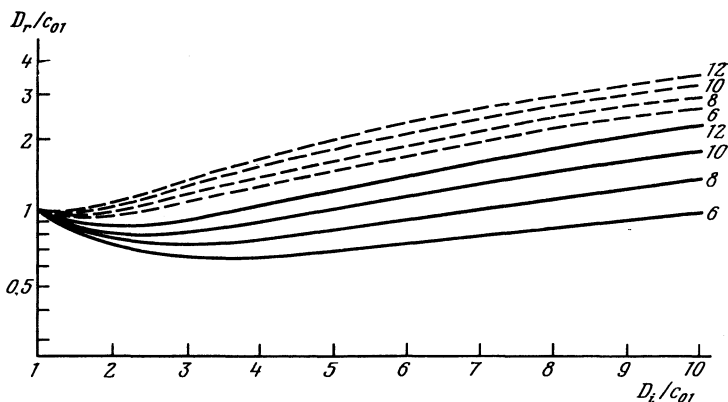


Fig. 6. Results of a numerical solution of the problem of reflection of a shock wave from the air-plasma boundary. The family of continuous curves corresponds to the air temperature of  $T_{02} = 1500$  K, whereas the dashed curves correspond to  $T_{02} = 300$  K. The temperature  $T_{01}$  is given alongside each curve in thousands of degrees Kelvin.

extended also to other forms of plasma. Improvements in the method may arise from studies of shock waves emerging across the contact boundary into air (this can be done, for example, by shadow photography) and comparing it with other well-known diagnostic methods.

The mechanisms responsible for the low-threshold breakdown of air by picosecond laser pulses, observed in our experiments, also deserve further study.

In conclusion, the authors express their deep gratitude to Academician A. M. Prokhorov for his interest in this investigation and for valuable comments made in discussions.

<sup>1</sup>Such giant peaks have a fine time structure (see §2).

<sup>2</sup>A typical spike duration in Ref. 8 was about 20 psec.

<sup>1</sup>V. A. Batanov, F. V. Bunkin, A. M. Prokhorov, and V. B. Fedorov, *Zh. Eksp. Teor. Fiz.* **63**, 1240 (1972) [*Sov. Phys. JETP* **36**, 654 (1973)].

<sup>2</sup>S. I. Anisimov, Ya. A. Imas, G. S. Romanov, and Yu. V. Khodyko, *Deistvie izlucheniya bol'shoi moshchnosti na metally* (Effects of High-Power Radiation on Metals), Nauka, M., 1970.

<sup>3</sup>V. A. Batanov, D. A. Dement'ev, A. N. Malkov, A. M. Prokhorov, and V. B. Fedorov, *Zh. Eksp. Teor. Fiz.* **77**, 2186 (1979) [*Sov. Phys. JETP* **50**,

1049 (1979)].

<sup>4</sup>A. J. Alcock and M. C. Richardson, *Phys. Rev. Lett.* **21**, 667 (1968).

<sup>5</sup>S. D. Kaitmazov, A. A. Medvedev, and A. M. Prokhorov, *Dokl. Akad. Nauk SSSR* **180**, 1092 [*Sov. Phys. Dokl.* **13**, 581 (1968)].

<sup>6</sup>B. Z. Gorbenko, Yu. A. Drozhbin, S. D. Kaitmazov, A. A. Medvedev, A. M. Prokhorov, and A. M. Tolmachov, *Dokl. Akad. Nauk SSSR* **187**, 772 (1969) [*Sov. Phys. Dokl.* **14**, 764 (1970)].

<sup>7</sup>V. A. Batanov and V. P. Gorkovskii, Preprint No. 124 (in Russian), Lebedev Physics Institute, Academy of Sciences of the USSR, Moscow (1981).

<sup>8</sup>A. N. Malkov, A. M. Prokhorov, V. B. Fedorov, and I. V. Fomenkov, *Pis'ma Zh. Eksp. Teor. Fiz.* **33**, 630 (1981) [*JETP Lett.* **33**, 615 (1981)].

<sup>9</sup>V. A. Batanov, V. A. Bogatyrev, N. K. Sukhodrev, and V. B. Fedorov, *Zh. Eksp. Teor. Fiz.* **64**, 825 (1973) [*Sov. Phys. JETP* **37**, 419 (1973)].

<sup>10</sup>W. D. Williams and J. W. L. Lewis, *AIAA J* **13**, 1269 (1975).

<sup>11</sup>A. I. Barchukov, F. V. Bunkin, V. I. Konov, and A. M. Prokhorov, *Pis'ma Zh. Eksp. Teor. Fiz.* **17**, 413 (1973) [*JETP Lett.* **17**, 294 (1973)].

<sup>12</sup>V. A. Batanov, K. S. Gochelashvili, B. V. Ershov, A. N. Malkov, P. I. Kolisnichenko, A. M. Prokhorov, and V. B. Fedorov, *Pis'ma Zh. Eksp. Teor. Fiz.* **20**, 411 (1974) [*JETP Lett.* **20**, 185 (1974)].

<sup>13</sup>L. D. Landau and E. M. Lifshitz, *Mekhanika sploshnykh sred*, Gostekhnizdat, M., 1953 (Fluid Mechanics, Pergamon Press, Oxford, 1959).

Translated by A. Tybulewicz